PASJ: Publ. Astron. Soc. Japan **46**, L157–L161 (1994)

Detection of X-Rays from SN 1993J with ASCA

Yoshiki KOHMURA
Institute of Physical and Chemical Research (RIKEN), Hirosawa, Wako, Saitama 351-01
E-mail (YK) kohmura@srsunix.riken.go.jp

Hajime INOUE, Takashi AOKI, Manabu ISHIDA, Masayuki ITOH, Taro KOTANI, and Yasuo TANAKA
Institute of Space and Astronautical Science, 3-1-1 Yoshinodai, Sagamihara, Kanagawa 229

Yoshitaka ISHISAKI, Kazuo MAKISHIMA, and Kyoko MATSUSHITA
Department of Physics, The University of Tokyo, Bunkyo-ku, Tokyo 113

Eric GOTTHELF
NASA/GSFC, Code 666, Greenbelt, MD 20771, USA

George RICKER
Center for Space Research, Massachusetts Institute of Technology, Cambridge, MA 02139, USA

and

Yoshiyuki TSUSAKA
Department of Physics, Nagoya University, Chikusa-ku, Nagoya 464-01

(Received 1994 March 18; accepted 1994 May 14)

Abstract

ASCA observed SN 1993J seven times between April 5 and October 24 in 1993. The 1–10 keV luminosity 10 d after the explosion was $(15\pm4)\times10^{39}$ erg s^{-1} and decreased monotonicly to $(1.3\pm0.4)\times10^{39}$ erg s^{-1} 210 d after the explosion, when a distance of 3.6 Mpc was assumed. The hardness ratio (2–10 keV/0.5–2 keV) significantly decreased during the course of the observations. The spectrum obtained from a sky region including not only SN 1993J but also the nearby X-ray source clearly shows an iron emission line. The correlation between the iron line flux with the SN 1993J flux suggests that the iron line emission originated in SN 1993J. These observational results are discussed in the context of thermal X-ray emission from a hot region behind the shock due to the collision of the supernova ejecta with the pre-supernova stellar wind.

Key words: Stars: evolution — Supernovae: general — Supernovae: individual (SN 1993J) — X-rays: stars

1. Introduction

SN 1993J was discovered in the nearby galaxy M81 (NGC 3031) on 1993 March 28, in the early rising phase (Garcia 1993). By the detection of clear hydrogen Balmer lines, SN 1993J was initially identified as a type II supernova (Filippenko 1993; Garnavich, Hong 1993; Taniguchi et al. 1993). The strong hydrogen line feature, however, gradually decayed and instead the He line feature became apparent, which is usually typical of a type Ib supernova (Filippenko et al. 1993). SN 1993J is now classified as type IIb (Nomoto et al. 1993; Woosley et al. 1994).

In the optical band, SN 1993J quickly reached an initial maximum, declined in about 5 d, rose to a second maximum in 10–15 d (depending on the wavelength), and declined again. The first and second maxima are interpreted as due to shock heating of the supernova ejecta and as due to the radio-active decay of ^{56}Co, respectively (Nomoto et al. 1993; Podsiadlowski et al. 1993; Shigeyama et al. 1994; Wheeler et al. 1993).

The first detection of the radio emission was carried out at 22.5 GHz by the VLA only 5d after the optical outburst (Weiler et al. 1993). This was much sooner after the explosion than in the previous supernovae which suggested the existence of a dense circumstellar matter and ejecta with large expansion velocity. From the radio light curve, Lundqvist (1993) suggested that the density profile of the circumstellar matter (CSM) is flatter than the r^{-2} expected from a constant-velocity wind model.

X-rays were also detected very soon after the optical outburst. ROSAT (Zimmermann et al. 1993) and ASCA (Tanaka 1993) successively detected X-rays from SN 1993J only 6 and 8 days after the explosion, respectively. These X-ray detections are much sooner after the explosion than those in the previous X-ray detected SN events: two weeks after the explosion from SN 1980K (Canizares et al. 1982); a half year after the explosion from SN 1987A (Dotani et al. 1987; Sunyaev et al. 1987).

Table 1. Observational log of SN 1993J in 1993.

No.	Start m/d h:m	End m/d h:m	Exposure (ks)
1	04/05 07:45	04/06 01:04	34
2	04/07 00:55	04/08 00:53	35
3	04/16 22:30	04/17 17:30	58
4	04/25 14:10	04/25 21:31	14
5	05/01 22:16	05/02 14:11	25
6	05/18 20:47	05/19 20:30	44
7	10/24 16:00	10/25 14:20	44

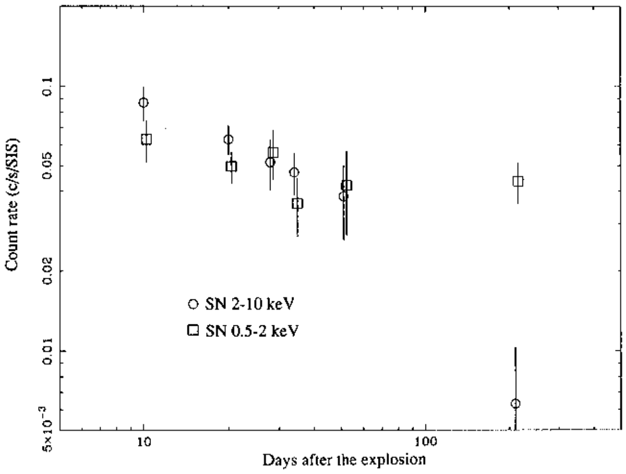

Fig. 1. X-ray lightcurve of SN 1993J in two energy bands as determined through the one-dimensional projection analysis using the SIS images. Open squares and open-circles represent count rates in 0.5–2 keV and 2–10 keV band, respectively. SIS-S0 and SIS-S1 data are averaged.

In this letter, we briefly report the results of the early observations of SN 1993J with ASCA.

2. Result

Following the optical discovery, the first ASCA observation of SN 1993J was carried out on 1993 April 5. Observations were repeated almost once every week until mid May. After the long interval from the end of May to mid October during which ASCA could not point its X-ray telescope (XRT; Serlemitsos et al. 1994) to SN 1993J due to the sun-angle constraint of the satellite (Tanaka et al. 1994), ASCA again observed the target on 1993 October 24. The log of the observations analyzed here is summarized in table 1. The GIS data were always taken in the PH normal mode (Ohashi et al. 1991), whereas the SIS data were obtained in the 4-CCD mode except during the sixth observation in May 18–19 where data were acquired in the 2-CCD mode (Burke et al. 1991).

2.1. Source Identification

There were always three X-ray sources in the SIS field of view during the observations shown in table 1. Comparing the source positions with those of the X-ray sources detected with the Einstein IPC (Fabbiano 1988), two of the three sources detected in the SIS field were identified with the two IPC sources, X-5 at the nucleus of M81 and X-6 which is probably a bright X-ray binary in M81. The third source is separated by about 3′ from X-5 and by about 1′ from X-6; there was no IPC source at that position. The coordinates of the source were calculated relative to those of the two IPC sources and were found to coincide with the optical position of SN 1993J (Hartwick et al. 1993) within 0.′1.

2.2. Light Curve

Although SN 1993J is clearly resolved in the SIS image, it heavily overlaps with X-6, and even X-5 produces considerable contamination in the SN 1993J region. This is because the XRT on board ASCA has a half power diameter of about 3′ (Serlemitsos et al. 1994).

The SN 1993J intensity has been isolated through one-dimensional image fitting (Kohmura 1994). That is, a rectangular box of $1' \times 2'$ containing SN 1993J and X-6 is defined on the SIS image, so that the box is elongated along the vector connecting SN 1993J and X-6. X-rays falling inside the box are projected across the box to produce a one-dimensional intensity profile, in which SN 1993J and X-6 appear as two peaks. After removing the contamination from X-5 (utilizing the image in the region symmetrically placed with respect to X-5), the profile is fitted with a model profile, which consists of two template sources with fixed positions representing SN 1993J and X-6. The template simulates the projected point-spread function of the XRT. Intensities of the two sources in the model are adjusted so as to give the best fit to the data.

Figure 1 shows X-ray lightcurves of SN 1993J thus obtained in the 0.5–2 keV and 2–10 keV bands, displayed in a log–log plot as a function of time t after the explosion. The figure reveals a roughly monotonic intensity decline, and a significant spectral softening towards 210 d after the explosion. The decline can be approximated as $\propto t^{\gamma}$, with $\gamma = -0.10^{+0.07}_{-0.16}$ and $\gamma = -0.71^{+0.15}_{-0.17}$ in the 0.5–2 keV and 2–10 keV bands, respectively. The larger value of γ in the harder band indicates spectral softening. These results generally agree with the ROSAT measurements.

Table 2. Spectral parameters of SN 1993J*

Date†	Photon index			Temperature	
	$N^{\ddagger}_{\mathrm{H},21} = 0.6$	$N_{\mathrm{H},21} = 3$	WA§	$N_{\mathrm{H},21} = 0.6$	$N_{\mathrm{H},21} = 3$
10	0.71 ± 0.13	1.02 ± 0.14	$1.2^{+0.2}_{-0.1}$	—♯	—
20	0.79 ± 0.10	1.11 ± 0.10	1.3 ± 0.1	—	—
28	$1.10^{+0.29}_{-0.21}$	$1.44^{+0.31}_{-0.23}$	+++♭	> 30	14(> 5)
34	$0.76^{+0.30}_{-0.23}$	$1.07^{+0.32}_{-0.24}$	+++	—	>20
51	$1.11^{+0.56}_{-0.35}$	$1.45^{+0.60}_{-0.38}$	+++	>6	14(>3)
210	$2.91^{+0.99}_{-0.52}$	$3.38^{+1.06}_{-0.56}$	+++	$1.7^{+1.4}_{-1.1}$	$1.1^{+1.0}_{-0.8}$

* The parameters are evaluated from the light curves of figure 1. Three cases are assumed for the absorber, that is, a cold aborber with column density $N_{\mathrm{H}} = 0.6 \times 10^{21}$ H atoms cm^{-2}, a cold absorber with $N_{\mathrm{H}} = 3 \times 10^{21}$ H atoms cm^{-2} (subsection 2.3), and a warm absorber with $\xi = 80$ (subsection 2.4).

† The day after explosion (1993 March 28), represented as t in this paper.

‡ The assumed column density in units of 10^{21} H atoms cm^{-2}.

§ The case of a warm absorber, with $\xi = 80$ and $N_{\mathrm{H}} = 6 \times 10^{22}$ H atoms cm^{-2} (for $t = 10$ d) or 3×10^{22} H atoms cm^{-2} (for $t = 20$ d). For the assumed value of N_{H}, see section 3.

♯ The spectral hardness is too large to be represented by thermal Bremsstrahlung.

♭ Poor statistics for analysis.

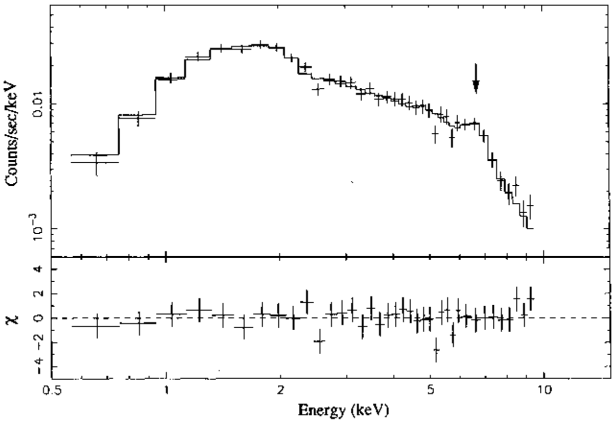

Fig. 2. X-ray spectrum by the GIS-S2 for the SN plus X-6 region, taken on April 5 fitted with a single power-law model with low-energy absorption and an additional single emission line centered at about 6.7 keV with the width of 0.3 keV. For the examination of the iron line, we model the overall continuum simply with a single power-law modified with photoelectirc absorption, rather than explicitly considering contributions from the three sources.

2.3. *Broad-Band Spectra*

If a simple spectral form, e.g., power-law or thermal Bremsstrahlung, is assumed for the SN 1993J spectrum, the two-band light curves in figure 1 can be translated into the evolution of photon index or Bremsstrahlung temperature. Table 2 tabulates the spectral parameters of SN 1993J thus estimated, in which the absorber was assumed to be neutral with the the photoelectric absorbing column density, N_{H}, of either 3×10^{21} or 6×10^{20} H atoms cm^{-2}. These values of N_{H} correspond to those determined with ROSAT in 1993 April and November, respectively (Zimmermann et al. 1994; Zimmermann et al. 1993). If the absorbing column is neutral with such small absorbing column density, then the spectrum of SN 1993J in the very early phase is too hard to be interpreted in terms of thermal emission (see table 2).

In order to estimate N_{H} based on the ASCA data themselves, the same analysis as was done to derive figure 1 was repeated in three broad energy bands, 0.5–1.5, 1.5–2.5, and 2.5–10.0 keV. By comparing intensities in these three energy bands, the absorbing column density for SN 1993J has been estimated to be $N_{\mathrm{H}} < 3 \times 10^{21}$ H atoms cm^{-2} for the April 17 observation which has the best statistics. This result agrees with the ROSAT measurements. The analysis also indicates that the X-6 spectrum can be represented with a Bremsstrahlung model with temperature $kT \geq 4$ keV, absorbed with $N_{\mathrm{H}} = (3 - 5) \times 10^{21}$ H atoms cm^{-2}.

2.4. *Multi-Channel Spectra*

Analysis of full-resolution spectra has been performed using the GIS data which has better statistics (Kohmura 1994). Figure 2 shows an example of GIS-S2 spectrum on April 5, accumulated over a region of radius 1.′5 centered on SN 1993J and X-6. The spectrum contains flux from both SN 1993J and X-6, and a small fraction of the X-5 flux. Clear evidence of iron K-line emission is seen at about 7 keV, which was significant in early observations but became gradually inconspicuous later. Because of this time behavior the iron line can be attributed to SN 1993J rather than to X-6. The line center energy of 6.7 ± 0.2 keV indicates that it is emission from highly ionized iron atoms. (Errors here represent the 90% confidence range.) The iron emission line is less significant in the SIS spectra but the equivalent width (relative to the SN 1993J continuum) of 500–800 eV and the width of 0.3 ± 0.3 keV were consistent with both the GIS and the SIS spectra obtained on April 7. The iron line center energy and its equivalent width are consistent with being constant in time, though the statistics are poor.

The GIS spectra have been fitted with a spectral model consisting of a Gaussian line and three continuum components; a power-law with absorption for SN 1993J, a $kT = 4.6$ keV Bremsstrahlung absorbed with $N_{\mathrm{H}} = 4 \times 10^{21}$ H atoms cm^{-2} for X-6, and a power-law of photon index 1.7 without absorption for the contamination from X-5. Levels of the X-6 and X-5 components are fixed to the values indicated by the broad-band analysis. The fit has been successful, and the obtained result, the photon-index ~ 1 and the absorbing column density $N_{\rm H} < 3 \times 10^{21}$ H atoms cm^{-2} for SN 1993J, is consistent with that derived in subsection 2.3.

In order to study possible X-ray photo-ionization effects in the circumstellar matter (CSM) around SN 1993J, the SN 1993J spectrum is next modeled by a power-law of photon index 1.3, modified with a "warm" (partially photo-ionized) absorber calculated using the CLOUDY code (Ferland 1991). Acceptable fits to the GIS spectra in April have been obtained with an ionization parameter ξ (e.g., Kallman, McCray 1982; see next section) of about 80 and the total CSM column density $N_{\rm H}^{\rm tot}$ in the range 10^{22-23} H atoms cm^{-2} on $\simeq 20$ d after the explosion. (The fit chi-squared is slightly, but not significantly, better than was achieved by the power-law plus cold absorber modeling.) The inferred photo-ionization can reconcile the presence of a relatively thick CSM with the lack of significant low-energy absorption in the ROSAT and ASCA spectra. Furthermore, as listed in table 2, correction for the warm absorption makes the intrinsic SN 1993J spectrum significantly steeper, such that the thermal interpretation becomes valid. These considerations indicate that the CSM is very likely to have been actually photo-ionized significantly in the early phase following the explosion.

3. Discussion

The origin of the X-ray emission from SN 1993J is consistent with type II supernova models (Chevalier 1982; Suzuki et al. 1993) where hot plasma is generated behind the front shock by the collision of the supernova ejecta with the CSM. The presence of the iron line with an energy above 6.5 keV indicates the existence of highly ionized iron (Fe XX–XXVII), in other words, the presence of thin hot plasma either in SN 1993J or in X-6. X-6 seems, however, to be an X-ray binary in the M81 galaxy and such a source does not usually show a prominent iron emission line with an equivalent width of more than a hundred eV (e.g., Hirano et al. 1987). The gradual decrease of the iron line emission in association with the luminosity decrease of SN 1993J indicates that SN 1993J is the more likely origin of the iron emission line.

We roughly estimated the luminosity of SN 1993J in the 1–10 keV range on the assumption of a power-law spectrum, an absorbing column density, $N_{\rm H}$, of 6×10^{20} H atoms cm^{-2} (Zimmermann et al. 1994), and a source distance of 3.6 Mpc (Freedman et al. 1994). The luminosity thus obtained in the 1–10 keV range was $(15\pm4)\times10^{39}$ erg s^{-1}, $(10.4\pm0.4)\times10^{39}$ erg s^{-1}, and $(1.3\pm0.4)\times10^{39}$ erg s^{-1} after 7, 20, and 210 d of the explosion, respectively. The luminosity decreased in time as $\propto t^{(-0.79\pm0.15)}$, where t represents time after the explosion. The plasma parameters of the matter behind the front and reverse shock were approximated by Chevalier (1982) on the assumption that the radial density profiles are $n \propto r^{-2}$ and $r^{-\alpha}$ for the circumstellar matter and the supernova ejecta, respectively. (Chevalier 1982 regarded α to be in the range of 7–12.) In this standard model, the two shock luminosities both decrease in time as $t^{-(\alpha-3)/(\alpha-2)}$, which is consistent with our observational result.

Two observational facts, however, call into question thermal emission from the shocked region as the source of the observed emission. One is the high hardness ratio of the 2–10 keV flux to the 0.5–2 keV flux on $t \simeq 10$ d (subsection 2.3); the other is the increase in the absorbing column density observed by ROSAT (Zimmermann et al. 1994; Zimmermann et al. 1993). The CSM surrounding the shock region is the most likely origin of the X-ray absorption. If we assume a density profile for the CSM as $n_{\rm CSM} \propto r^{-2}$, the total column density, $N_{\rm H}^{\rm tot}$, of the CSM surrounding the shock front will depend on the radius of the shock front ($r_{\rm f}$) as $N_{\rm H}^{\rm tot} = \int_{r_{\rm f}}^{\infty} n_{\rm CSM}(r)dr \simeq n_{\rm CSM}(r_{\rm f})r_{\rm f} \propto r_{\rm f}^{-1}$. Thus, $N_{\rm H}^{\rm tot}$ will decrease in time as $\propto t^{-1}$ (neglecting the deceleration of the shock front), while the ROSAT observation has shown an increase in $N_{\rm H}$ with time.

These contradictions could be resolved by introducing partial ionization of the CSM by the X-ray irradiation from the supernova. Assuming the total column density of the CSM, $N_{\rm H}^{\rm tot}$, is 3×10^{21} H atoms cm^{-2} on $t \simeq 200$ d (Zimmermann et al. 1993), it could be as high as $\simeq 3\times10^{22}$ H atoms cm^{-2} on $t \simeq 20$ d. Since $N_{\rm H}^{\rm tot} = n_{\rm CSM}(r_{\rm f})r_{\rm f}$, the ionization parameter $\xi \equiv L/nr^2$ (e.g., Kallman, McCray 1982) is estimated to be as high as 80 by substituting $L \simeq 10^{40}$ erg s^{-1}, $n_{\rm CSM}(r_{\rm f})r_{\rm f} \simeq 3\times10^{22}$ H atoms cm^{-2} and $r_{\rm f} \simeq V_{\rm ex}t \simeq 4\times10^{15}$ cm in $\xi = L/n_{\rm CSM}(r_{\rm f})r_{\rm f}^2$ (We assumed $V_{\rm ex} \simeq 2.4\times10^4$ km s^{-1} after Marcaide et al. 1994). When $\xi \simeq 80$, such low z material as Carbon will be fully ionized (Kallman, MacCray 1982) which may have made the absorbing column density $N_{\rm H}$ evaluated from the ROSAT observation during April and May (Zimmermann et al. 1994) much smaller than the total amount. On the other hand, the partially ionized elements such as Helium-like and Hydrogen-like Oxygen or those of Neon should contribute to the X-ray absorption above their K-edge energies (0.74, 0.87, 1.20, and 1.36 keV, respectively), and the observed X-ray flux in the energy range of 0.5 to 2 keV would have been reduced by such absorption. Thus the high hardness ratio obtained by ASCA in April could be reconciled with the thermal spectrum by correcting for the larger effect of absorption below 2 keV. In fact, the spectrum on $t \simeq 20$ d is consistent with a thermal bremsstrahlung with temperature of a few tens of keV when $\xi \simeq 80$ and

$N_{\rm H}^{\rm tot} = 10^{22}$–$10^{23}$ H atoms cm^{-2} (see subsection 2.4).

Although the contradiction of the observed hardness ratio with the thermal spectrum can be resolved by introducing the effect of a warm absorber, the temperature is still as high as a few tens of keV on $t \simeq 20$ d. The temperature, however, decreased to about 1 keV on $t \simeq 200$ d. This rapid temperature drop is still difficult to explain in the context of the thermal emission from the shock-heated hot region as simulated by Suzuki et al. (1993).

The authors are grateful to Drs. W. Lewin, D. Helfand, K. Nomoto, and Mr. T. Suzuki for their useful discussions and suggestions.

References

Burke B.E., Mountain R.W., Harrison D.C., Bautz M.W., Doty J.P., Ricker G.R., Daniels P.J. 1991, IEEE Trans. ED-38, 1069

Canizares C.R., Kriss G.A., Feigelson E.D. 1982, ApJL 253, L17

Chevalier R.A. 1982, ApJ 259, 302

Dotani T., Hayashida K., Inoue H., Itoh M., Koyama K., Makino F., Mitsuda K., Murakami T. et al. 1987, Nature 330, 230

Fabbiano G. 1988, ApJ 325, 544

Ferland G.J. 1991, The Ohio State University, Astronomy Department Internal Report, "CLOUDY 80.05"

Filippenko A.V. 1993, IAU Circ. No.5731

Filippenko A.V., Matheson T., Ho L.C. 1993, ApJL 415, L103

Freedman W.L., Hughes S.M., Madore B.F., Mould J.R., Lee M.G., Stetson P., Kennicutt R.C., Turner A. et al. 1994, ApJ 427, 628

Garcia F. 1993, IAU Circ. No.5731

Garnavich P., Hong B.A. 1993, IAU Circ. No.5731 (corrigendum: IAU Circ. No.5733)

Hartwick F.D.A, Balam D.D., Zurek D., Robb R.M. 1993, IAU Circ. No.5731

Hirano T., Hayakawa S., Nagase F., Masai K., Mitsuda K. 1987, PASJ 39, 619

Kallman T.R., MacCray R. 1982, ApJS 50, 263

Kohmura Y. 1994, Ph. D. Thesis, University of Tokyo

Lundqvist P. 1993, Circumstellar Media in the Late Stages of Stellar Evolution, The 34th Herstmonceux Conference, ed R. Clegg, P. Meikle, I. Stevens (Cambridge University Press, Cambridge) in press

Marcaide J.M., Alberdi A., Elósgui P., Guirado J.C., Mantovani P., Pérez E., Ratner M.I., Rius A. et al. 1994, ApJL 424, L25

Nomoto K., Suzuki T., Shigeyama T., Kumagai S., Yamaoka H, Saio H. 1993, Nature 364, 507

Ohashi T., Makishima K., Ishida M., Tsuru T., Tashiro M., Mihara T., Kohmura Y., Inoue H. 1991 Proc. SPIE 1549

Podsiadlowski Ph., Hsu J.J.L., Joss P.C., Ross R.R. 1993, Nature 364, 509

Serlemitsos P., Jalota L., Soong Y., Kunieda H., Tawara Y., Tsusaka Y., Suzuki H., Sakima Y. et al. 1994, PASJ submitted

Shigeyama T., Suzuki T., Kumagai S., Nomoto K., Saio H., Yamaoka H. 1994, ApJ 420, 341

Suzuki T., Kumagai S., Shigeyama T., Nomoto K., Yamaoka H., Saio H. 1993, ApJL 419, L73

Sunyaev R. et al. 1987, Nature 330, 227

Tanaka Y. 1993, IAU Circ. No.5753

Tanaka Y., Inoue H., Holt S.S. 1994, PASJ 46, L37

Taniguchi Y., Murayama T., Sato Y., Yadoumaru Y., Ohyama Y., Kosugi G., Yoshida M., Kurakami T. 1993, PASJ 45, L43

Weiler W. et al. 1993, IAU Circ. No.5752

Wheeler J.C., Barker E., Benjamin R., Boisseau J., Clocchiatti A., de Vaucouleurs G., Gaffney N., Harkness R.P. et al. 1993, ApJL 417, L71

Woosley S.E., Eastman R.G., Weaver T.A., Pinto P.A. 1994, ApJ 429, 300

Zimmermann H.U., Lewin W., Magnier E., Predehl P., Hasinger G., Pietsch W., Acshenbach B., Trümper J. et al. 1993, IAU Circ. No.5748

Zimmermann H.-U., Lewin W., Predehl P., Acshenbach B., Fabbiano G., Hasinger G., Lubin L., Magnier E. et al. 1994, Nature 367, 621